Scaling exponents of rough surfaces generated by the Domany-Kinzel cellular automaton

A. P. F. Atman,* Ronald Dickman,† J. G. Moreira‡
Departamento de Física, Instituto de Ciências Exatas, Universidade Federal de Minas Gerais, C. P. 702 30123-970, Belo Horizonte, MG, Brazil

(Received 24 September 2001; published 22 July 2002)

The critical behavior at the frozen-active transition in the Domany-Kinzel stochastic cellular automaton is studied via a surface growth process in $(1+1)$ dimensions. At criticality, this process presents a kinetic roughening transition; we measure the critical exponents in simulations. Two update schemes are considered: in the symmetric scheme, the growth surfaces belong to the directed percolation (DP) universality class, except at one terminal point. At this point, the phase transition is discontinuous and the surfaces belong to the compact directed percolation universality class. The relabeling of space-time points in the nonsymmetric scheme alters significantly the surface growth, changing the values of the critical exponents. The critical behavior of rough surfaces at the nonchaotic-chaotic transition is also studied using the damage spreading technique; the exponents confirm DP values for the symmetric scheme.

DOI: 10.1103/PhysRevE.66.016113 PACS number(s): 05.10.−a, 02.50.−r, 68.35.Ct, 68.35.Rh

I. INTRODUCTION

The one-dimensional Domany-Kinzel stochastic cellular automaton (DKCA) is a completely discrete system—temporally, spatially, and in its state space—with applications in physics, chemistry, biology, computer science, etc. [1,2]. The DKCA also attracts interest as a particle system affording a test of certain conjectures regarding nonequilibrium critical phenomena [3]. The DKCA has a unique absorbing (''vacuum'') state; its phase diagram presents a critical line separating this absorbing phase from an active phase. Models with one absorbing state have been conjectured to belong generically to the directed percolation (DP) universality class [4]. There is also good numerical evidence [3] that the critical behavior along the transition line in the DKCA belongs to the DP class, except at one of the terminal points, where the asymptotic behavior is known exactly and belongs to the compact directed percolation (CDP) universality class [1,5,6]. At this terminal point the transition is discontinuous and we have in fact two absorbing states: the vacuum and the completely filled state. Martins *et al.* [7] found a damage spreading transition line separating the active phase into a nonchaotic and a chaotic phase. There is numerical evidence that the critical behavior along this transition line also belongs to the DP class, as expected on the basis of universality [8]. It is important to distinguish this damage spreading transition, involving a *pair* of automata, from the frozen-active transition, that involves only *one* automaton. See the reviews by Hinrichsen [9,10] for a discussion of experimental realizations of directed percolation and the relation of growth models to DP.

The surface growth process generated by cellular automata (CA) was proposed by de Sales *et al.* [11] to study Wolfram's deterministic CA. These authors also used this process to identify the frozen-active phase transition in the DKCA [12], where they showed that the Hurst exponent H attains a maximum at the transition. Recently, Atman and Moreira [13] demonstrated that the growth exponent β_w also presents a cusp at criticality, and is more appropriate for detecting phase transitions than the method of de Sales *et al.* They used it to construct the DKCA phase diagram and conjectured that the growth exponent method also can be used to detect phase transitions in other kinds of models. Recently, Redinz and Martins [14] used the Hurst exponent method to find first- and second-order phase transitions in the q-state Potts model (for $q=1,3,5$, and 10). Bhattacharyya [15] studied the dynamic critical properties of a related one-dimensional probabilistic cellular automaton, using two different procedures to generate the surface growth process. One of them is identical to the growth process studied by de Sales *et al.* and belongs to DP universality class. Thus, the conjectures presented by Bhattacharyya [15], which imply DP-like scaling for this model are also valid here.

The procedure used by de Sales *et al.* [12] and by Bhattacharyya [15] transforms the spatiotemporal patterns generated by the DKCA to a solid-on-solid particle deposition. The nature of the resulting interface is an interesting open question since there are many recipes for mapping dynamical systems to interfaces, and in many cases the outcome is completely unknown *a priori*. The reason is that sometimes the interface turns out to have surface tension, and thus can be expected to be related to a known universality class, while in other cases there is no surface tension. At the critical line, the DKCA surface growth process exhibits kinetic roughening, and the critical exponents can be measured following the scaling concepts developed by Family and Vicsék [16]. Very recently, similar methods were used by Lauritsen and Alava [17] to study the Edwards-Wilkinson equation with columnar noise, by Vespignani *et al.* [18] to study sandpile models, and by Dickman and Muñoz [19], to study the contact process (CP).

In this work, we measure the scaling exponents at criticality in simulations, and compare them with known DP and CDP values. We use two different schemes to update the automaton, which lead to entirely different surface growth

*Email address: atman@fisica.ufmg.br
†Email address: dickman@fisica.ufmg.br
‡Email address: jmoreira@fisica.ufmg.br

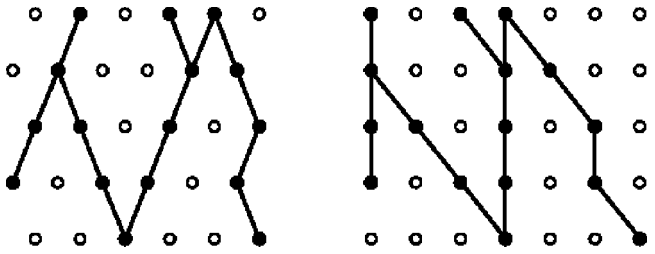

FIG. 1. Spatial representation of DKCA, in symmetric (left) and nonsymmetric (right) schemes, showing that the spatiotemporal patterns are identical in the two schemes, i.e., corresponding histories are identical.

scaling properties. In Sec. II, we define the DKCA, describe the two update schemes, and show how the surface growth process is generated, at the frozen-active and nonchaotic-chaotic transitions. In Sec. III, we present our numerical results and discuss the values obtained, comparing them with the predictions for the scaling exponents proposed by Bhattacharyya [15] and Dickman and Muñoz [19]. We discuss our conclusions in Sec. IV.

II. DKCA SURFACE GROWTH PROCESS

A. Model

The DKCA was proposed by Domany and Kinzel [1], who showed the existence of two phases: *active* and *frozen*. A more detailed study, using simulation, was performed by Martins *et al.* [7], in which a new phase within the active region—a *chaotic* phase—was discovered through the damage spreading technique.

The DKCA consists of a linear chain of L sites ($i=1,2,\ldots,L$), with periodic boundaries, where each site i has two possible states, conveniently denoted by $\sigma_i=0,1$. The state of the system at time t is given by the set $\{\sigma_i(t)\}$. In contrast to the deterministic CA studied by Wolfram [2], the DKCA is probabilistic: the rules for updating the system are given by conditional probabilities, which depend on the neighbors. We study two different schemes, one symmetric, the other nonsymmetric. The symmetric scheme is the original one proposed by Domany and Kinzel [1], while the nonsymmetric was used [20] to simplify the algorithm.

In the symmetric scheme, the process $\sigma_i(t)$ is defined on space-time points with $i+t$ *even*. The state of site i at time $t+1$ depends on $\sigma_{i-1}(t)$ and $\sigma_{i+1}(t)$ via the transition probability $P[\sigma_i(t+1)|\sigma_{i-1}(t),\sigma_{i+1}(t)]$, which takes the form $P(1|0,1)=P(1|1,0)=p_1$, $P(1|1,1)=p_2$, $P(1|0,0)=0$. Evidently, $P(0|\sigma_{i-1},\sigma_{i+1})=1-P(1|\sigma_{i-1},\sigma_{i+1})$.

In the nonsymmetric scheme, the process is defined on *all* space-time points. The state of site i at time $t+1$ depends on $\sigma_{i-1}(t)$ and $\sigma_i(t)$, rather than on $\sigma_{i-1}(t)$ and $\sigma_{i+1}(t)$, as in the symmetric scheme. The transition probability $P[\sigma_i(t+1)|\sigma_{i-1}(t),\sigma_i(t)]$ is identical to $P[\sigma_i(t+1)|\sigma_{i-1}(t),\sigma_{i+1}(t)]$ given above for the symmetric case.

It is easy to see that the two schemes are connected via a simple relabeling of space-time points (see Fig. 1). Consider, for example, a *history* h^S in the symmetric scheme, that is, a sequence of configurations $\{\sigma_i^S(t)\}$ for $t=0,\ldots,T$ (T finite), starting at $t=0$ with a finite number of active sites. Let the probability of this history, given the initial configuration, be $P[h^S|\{\sigma^S(0)\}]$. A history h^{NS} in the nonsymmetric scheme can be defined in the same manner. Note that there is a one-to-one correspondence between histories in the two schemes, given by

$$\sigma_i^{NS}(t)\equiv\sigma_{2i-t}^{S}(t). \tag{1}$$

Since the transition probabilities in the two schemes are identical, the probabilities of corresponding histories are as well. To extend this correspondence to systems with periodic boundaries, we note that if the nonsymmetric system has L sites, then the corresponding symmetric one has $2L$ sites; in the mapping defined above, we now take $i^S=2i^{NS}-t(\mathrm{mod}\ 2L)$.

An immediate result of this correspondence is that all scaling properties (e.g., critical exponents), as well as nonuniversal properties (e.g., phase boundaries between frozen, active, and chaotic phases in the p_1-p_2 plane), are identical in the two schemes. Corresponding histories naturally look different in the two schemes: the nonsymmetric scheme represents a rotating frame of reference in which, moreover, distances are rescaled by a factor of 1/2. Thus, for $p_1=1/2$ and $p_2=1$, an interface between domains of 1's and 0's executes an unbiased random walk in the symmetric scheme, while in the nonsymmetric case such an interface has a mean velocity of 1/2. The ''light cone'' $i=\pm t$ in the symmetric scheme becomes the pair of lines $i=0$ and $i=t$ in the nonsymmetric case. As will be seen below, this difference in frames of reference has important consequences for the surface dynamics in the nonsymmetric scheme.

Depending on the values of the parameters (p_1,p_2), the asymptotic ($t\to\infty$) state of the system is either *frozen*, with all sites having value 0, or has a finite fraction of sites with value 1, the *active* state. This is a second-order phase transition, characterized by the critical exponents of the DP universality class.

B. Interface representation

The surface growth process consists in accumulating (summing) all the values assumed by the variables $\sigma_i(\tau)$ over the first t time steps:

$$h_i(t)\equiv\sum_{\tau=0}^{t}\sigma_i(\tau). \tag{2}$$

The differences between the schemes become explicit at this point. In Fig. 2, we show the temporal evolution of the automaton and the profiles generated by the accumulation method, close to criticality ($p_2=0.5,p_1=0.75$), in each scheme. It is evident that the two schemes lead to entirely different profiles. (In this figure, we choose an initial condition of a single active site, to highlight the evolution of the automaton and profiles.)

Thus, we obtain growth processes, the nature of whose correlations can be investigated through the analysis of the roughness $w(L,t)$ [21], defined by

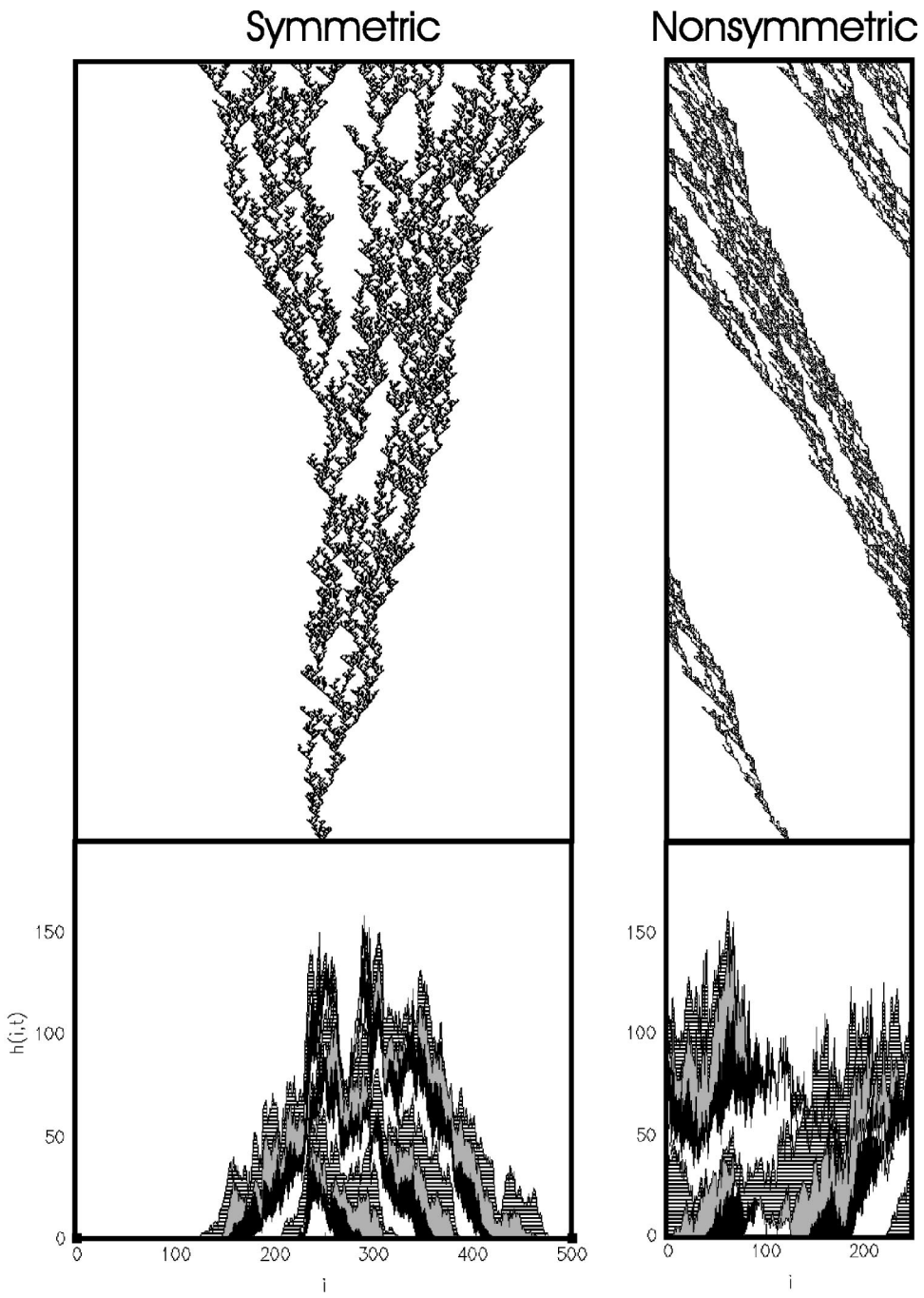

FIG. 2. Interface representation generated by spatiotemporal patterns of the DKCA with different update schemes: the symmetric scheme is shown on the left and the nonsymmetric on the right. Upper panels: spatiotemporal patterns of the automata. Black sites are active; time increases upward. Lower: Interface representation of the patterns shown above. Here, the *y* axis corresponds to the height $h(i,t)$ of the profiles [see Eq. (2)], and the *x* axis to the lattice positions *i*. The fill color is changed after every 50 time steps to highlight the profile roughness evolution. System size $L=500$ for the symmetric and $L=250$ for the nonsymmetric; 900 time steps are shown. Both systems are very close to criticality ($p_2=0.5$, $p_1=0.75$), in the active phase.

$$w^2(L,t)=\frac{1}{L}\left\langle \sum_{i=1}^{L}[h_i(t)-\overline{h}(t)]^2 \right\rangle, \tag{3}$$

where $\overline{h}(t)$ is the mean value of $h_i(t)$ at time t and the brackets $\langle\cdots\rangle$ denote an average over realizations.

We expect that $w(L,t)$ has the scaling form [16]

$$w(L,t)\sim L^{\alpha} f\left(\frac{t}{L^z}\right), \tag{4}$$

where $f(u)$ is a universal scaling function, α is the roughness exponent, $z=\alpha/\beta_w$ is the dynamic exponent, and β_w is the growth exponent. The function $f(u)=\text{const}$, at large times ($t\gg L^z$), and $f(u)\sim u^{\beta_w}$ at short times ($t\ll L^z$). So at short times, we expect $w(t)\sim t^{\beta_w}$; we measure β_w from the slope of the log-log plot of $w(L,t)$ vs t. At large times, the roughness saturates and becomes L dependent: $w(L,\infty)\sim L^{\alpha}$. The crossover time $t_{\times}$ between these two regimes grows as $t_{\times}\sim L^z$. The exponents α and z are defined in the frozen phase just at the transition line. In the active phase, the roughness does not saturate, growing instead as $w(L,t)\sim t^{1/2}$, corresponding to uncorrelated growth [13]. Thus, the relations above, used to measure the scaling exponents, are valid just at criticality for the DKCA.

The profiles have self-affine properties quantified by the Hurst exponent H, defined via

$$W(\epsilon) \sim \epsilon^H, \tag{5}$$

where $W(\epsilon)$ is the width of the interface on length scale ϵ. We measure the Hurst exponent H in a profile generated very close to the transition. We apply the method introduced by Moreira *et al*. [22], valid for self-affine profiles, that consists in measuring the roughness around the straight line determined by a least-squares fit to a segment of the profile. The roughness $W(L,\epsilon,t)$, at the scale ϵ, is given by

$$W(L,\epsilon,t) = \frac{1}{L}\sum_{i=1}^{L} w_i(\epsilon,t), \tag{6}$$

where the local roughness $w_i(\epsilon,t)$ is defined by

$$w_i^2(\epsilon,t) = \frac{1}{2\epsilon+1}\sum_{j=i-\epsilon}^{j=i+\epsilon} \{h_j(t) - [a_i(\epsilon)x_j + b_j(\epsilon)]\}^2,$$

where $a_i(\epsilon)$ and $b_i(\epsilon)$ are the linear fitting parameters to the profile on the interval $[i-\epsilon, i+\epsilon]$ centered at site i.

C. Damage spreading

Martins *et al.* [7] used the damage spreading technique to show that the active phase of the DKCA in fact consists of two phases, chaotic and nonchaotic. The order parameter of this transition is the difference between two replicas started with different initial configurations. One allows the system to evolve until it attains a stationary state, and then a replica of the configuration is created with some sites altered (damage). The two replicas, one with state $\sigma_i(t)$ and the other with state $\varrho_i(t)$, evolve with the same sequence of random numbers, and the difference between the configurations

$$\Gamma_i(t) = |\sigma_i(t) - \varrho_i(t)|,$$

is measured. The fraction of sites in the two replicas with $\sigma_i \neq \varrho_i$ is called the Hamming distance, defined as

$$D_H(t) = \frac{1}{L}\sum_i \Gamma_i(t).$$

The stationary Hamming distance is null in the nonchaotic phase and positive in the chaotic phase.

To study the chaotic-nonchaotic boundary, we use a slightly different method, where the difference between the two automata is used to generate the surface growth process, as we did in the accumulation method

$$h_i(t) = \sum_{\tau=0}^{t} \Gamma_i(\tau). \tag{7}$$

Thus, the profile generated by the difference between the replicas behaves exactly as the profiles generated in the frozen-active boundary: the roughness reaches a stationary value in the nonchaotic phase and grows indefinitely in the chaotic phase. This behavior can be understood if we note that the difference between the replicas vanishes in the nonchaotic phase, which implies no contribution to the height $h_i(t)$, and is positive in chaotic phase, implying steady growth in the height.

In order to preserve the stationary density of active sites we generate a ''rotation'' damage at a certain time t_0, in which the replica is rotated 180° with respect to the original system, that is $\varrho(i,t_0) = \sigma(i+L/2,t_0)$, subject to the periodic boundary condition.

D. Theoretical descriptions

One of the first theoretical analyses of critical growth exponents in the DP universality class was presented by Kértesz and Wolf [23], who considered a polynuclear growth model. Theoretical descriptions of surface growth scaling at absorbing-state phase transitions were proposed by Bhattacharyya [15], and Dickman and Muñoz [19]. Bhattacharrya proposed an analytical treatment in analogy to the random deposition (RD) process. We clarify that this is not a general description, being valid only at criticality. Considering an initial disordered state, the growth process can be described by a continuum equation, very similar to the RD process:

$$\frac{\partial h(x,t)}{\partial t} = F + \eta(x,t) \quad \text{(RD)}, \tag{8}$$

where F is the average number of deposited particles and $\eta(x,t)$ corresponds to the white noise ($\langle \eta(x,t)\rangle = 0$) in the deposition.

The difference between the surface growth processes generated by DKCA and RD lies in the noise correlations. While RD involves spatially and temporally uncorrelated noise, the correlations in time and space developing in the DKCA appears in the noise fluctuations of the accumulation method. For values of $(p1,p2)$ away from the critical line (in the active phase), the correlation length ξ and correlation time τ of the DKCA are finite, which means that the noise in the deposition process is correlated over short ranges. In this limit the noise autocorrelation decays exponentially [21]:

$$\langle \eta(x,t), \eta(x',t')\rangle \sim e^{-|x-x'|/\xi} e^{-|t-t'|/\tau}. \tag{9}$$

Thus, the noise appears uncorrelated for times greater than τ, and the RD exponents are obtained in this limit. This behavior was confirmed in earlier simulations [13]. As we approach the transition line, ξ and τ increase, and it takes longer for the growth process to reach the RD limit. Finally, at the critical line, both ξ and τ diverge, and the correlations are long ranged represented by a power law decay of the noise autocorrelation [21]

$$\langle \eta(x,t), \eta(x',t')\rangle \sim |x-x'|^{-2\beta/\nu_\perp} |t-t'|^{-2\beta/\nu_\parallel}, \tag{10}$$

where β, $\nu_\perp$, and $\nu_\parallel$ are, respectively, the critical exponents for the order parameter, correlation length, and correlation time of the DKCA.

The value of the growth exponent β_w at the critical line can be derived from the continuum equation (8) and the noise (10); the height $h(x,t)$ can be obtained integrating Eq. (8),

$$h(x,t)=\int_0^t d\tau F+\int_0^t d\tau \eta(x,\tau). \tag{11}$$

If we now let $h(x,t)\rightarrow h(x,t)-Ft$, considering only the fluctuations around the mean height, we can write the mean-square roughness, which is the variance of $h(x,t)$, as

$$\mathrm{var}[h(x,t)]=\int_0^t d\tau\int_0^\tau dt'\langle \eta(x,\tau)\,\eta(x,t')\rangle. \tag{12}$$

Thus, using Eq. (10), making the change of variables $\omega=\tau-t'$, we obtain

$$w^2(t)\sim\int_0^t d\tau\int_{\omega_0}^\tau d\omega\,\omega^{-2\beta/\nu_\parallel}\sim\int_0^t d\tau(\omega^{1-2\beta/\nu_\parallel})_{\omega_0}^{\tau}\sim t^{2-2\beta/\nu_\parallel}.$$

(We take the lower limit of integration as $\omega_0\sim 1$, since Eq. (10) holds for $|t-t'|\gtrsim 1$, and the scaling behavior arises from the decay of correlations at large spatial and temporal separations.) This implies that the width for an infinite substrate, for the symmetric scheme, follows the power law:

$$w(\infty,t)\sim t^{1-\beta/\nu_\parallel}. \tag{13}$$

As it is believed that this transition belongs to the DP universality class, considering the exponent values furnished by Jensen [24], the value of growth exponent is expected to be

$$\beta_w=1-\frac{\beta}{\nu_\parallel}=1-\frac{0.276\,49}{1.733\,825}\simeq 0.8405.$$

For the nonsymmetric scheme, due the correspondence between histories in the two schemes described by Eq. (1), the height is defined by

$$h(x,t)=\int_0^t d\tau\eta(2x-\tau,\tau), \tag{14}$$

yielding to

$$\begin{aligned}\mathrm{var}[h(x,t)]&=\int_0^t d\tau\int_0^\tau dt'\langle \eta(2x-\tau,\tau)\,\eta(2x-t',t')\rangle\\&=\int_0^t d\tau\int_0^\tau d\omega\langle \eta(\phi-\omega,t'+\omega)\,\eta(\phi,t')\rangle,\end{aligned} \tag{15}$$

where $\phi=2x-t'$. Thus, using Eq. (10)

$$w^2(t)\sim\int_0^t d\tau\int_{\omega_0}^\tau d\omega|\omega|^{-2\beta(1/\nu_\parallel+1/\nu_\perp)}\sim t^{2-2\beta(1/\nu_\parallel+1/\nu_\perp)}.$$

This implies that the width for an infinite substrate, for the nonsymmetric scheme, increases as the following power of the time:

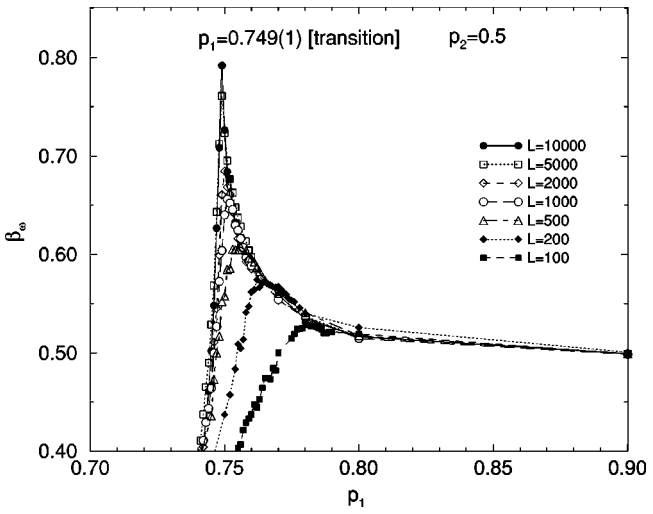

FIG. 3. Growth exponent β_w in the DKCA for several system sizes in the symmetric scheme. Note that β_w attains a maximum at the frozen-active transition and depends strongly on the system size. The transition point was chosen as the β_w value at system size $L=10\,000$, where we observe a sharp transition. In this example, $p_2=0.5$ and $p_1=0.749$.

$$w^{NS}(\infty,t)\sim t^{1-\beta(1/\nu_\parallel+1/\nu_\perp)}. \tag{16}$$

Considering [24] $\nu_\perp=1.096\,854$, the value of growth exponent in the nonsymmetric scheme is expected to be

$$\beta_w\simeq 0.588\,46,$$

in agreement with the value found in earlier simulations [13].

In previous work [13], Atman and Moreira showed that β_w attains a maximum at the phase transition (see Fig. 3), and measured its value along the transition line of the DKCA. This behavior of the exponent β_w in the vicinity of the phase transition can be understood as follows. The growth rate dh_i/dt at site i is proportional (in the frame of reference moving with the average velocity $d\langle h\rangle/dt$) to the *excess* activity at that site. Away from the critical point, the activity has a finite correlation length ξ and correlation time τ. Thus on scales much greater than ξ, τ, the noise driving the surface growth is uncorrelated, and this process falls in the RD class, with $\beta_w=1/2$. At the critical point, by contrast, ξ and τ diverge and we have instead the scaling relation $\beta_w=1-\theta$ [19], where the exponent θ is defined through the relation $\rho(t)\sim t^{-\theta}$ for the initial decay of the activity density ρ at the critical point, starting from $\rho(0)=1$. Since, in one dimension, $1-\theta>1/2$, we expect a jump in β_w at the phase boundary. In simulations of finite-sized systems, we expect not a discontinuity in β_w but a sharp peak at the transition–see Fig. 3 (very near to the critical point, $\xi>L$, so that independently fluctuating regions are not present in the simulation). Below the transition, the apparent value of $\beta_w\rightarrow 0$ due to the short lifetime of the activity. It is interesting to note that for the DP universality class, $1-\theta\simeq 0.55,0.27$, and 0 for $d=2,3$, and 4, respectively. Thus we should expect β_w to *decrease* at the phase boundary in $d=3$.

TABLE I. Summary of the scaling exponents values, $d=1$.

Previous work	α	β_w	z	H
DP	1.3286	0.8405	1.5808	0.643
CP (simulational) [19]	1.33	0.839(1)		0.63(3)
CA (simulational) [15]		0.837(11)		
CDP	2	1	2	1
Present work—symmetric scheme				
Frozen-active $p_2=0.5$	1.32(1)	0.82(2)	1.59(1)	0.61(3)
Frozen-active $p_2=1$	2.01(1)	0.99(1)	2.08(5)	0.99(2)
Nonchaotic-chaotic $p_1=1$	1.325(9)	0.81(1)	1.61(1)	0.60(3)
Nonchaotic-chaotic $p_2=0$	1.32(1)	0.78(2)	1.64(2)	0.61(3)
Present work—nonsymmetric scheme				
Frozen-active $p_2=0.5$	0.92(7)	*	1.58(4)	0.26(6)
Frozen-active $p_2=1$	0.984(7)	*	1.9(1)	0.501(25)
Nonchaotic-chaotic $p_1=1$	0.93(1)	*	1.67(2)	0.30(2)
Nonchaotic-chaotic $p_2=0$	0.910(7)	*	1.66(1)	0.28(3)

Since the saturation of surface width is forced by the DKCA, the crossover time $t_\times$ behaves exactly as in DP, and the dynamic exponent is given by

$$t_\times \sim L^z, \quad z=z^{DP}=\nu_\parallel/\nu_\perp \simeq 1.5808. \tag{17}$$

Thus, the roughness exponent at the criticality is given by

$$\alpha = z\beta_w \simeq 1.3286. \tag{18}$$

Dickman and Muñoz [19] studied the contact process using the surface growth representation. They demonstrated that the Hurst exponent shows clear signs of anomalous scaling ($\alpha > H$), but no evidence of multiscaling. They verified López' scaling relation [25]: $H=\alpha - z\kappa$. Here, $\kappa = 0.4336(4)$ is the exponent associated with the divergence of the mean-square height gradient in the continuum growth equation that describes the contact process and related models, such as DP. Inserting the known values in the relation above we have for the Hurst exponent in the DP class:

$$H=\alpha - z\kappa \simeq 0.643. \tag{19}$$

III. RESULTS

In Table I, we summarize our results for the scaling exponents at the frozen-active and nonchaotic-chaotic transitions, and compare them with the values for the DP and CPD universality classes.

To extract the exponent values from our simulation data, we used the relations $w(L,\infty)\sim L^\alpha$, valid at large times, $w(L,t)\sim t^{\beta_w}$, valid at short times and $t_\times(L)\sim L^z$. The results show a strong dependence on the scheme used—symmetric or nonsymmetric. In the simulations, we average 10 000, 5000, 2500, 1000, 500, 250, and 100 samples at the critical point (p_2^c, p_1^c) in systems with $L=50$, 100, 200, 500, 1000, 2000, and 5000 sites, respectively. The initial condition in these samples was random, with 50% of sites active.

The Hurst exponent was measured following the procedure explained in Sec. II B. The results, shown in Table I, represent an average over 100 random initial configurations in a system with $L=10\,000$. We observe a significant change in the value of the Hurst exponent depending on the scheme used to update the automaton: in the symmetric scheme, we have $H>1/2$, denoting a positive correlation in the profile; in the nonsymmetric scheme $H=0.25(3)$, denoting a negative correlation. This behavior can be understood considering the nonsymmetric scheme as a deposition over a moving reference frame, which implies a lateral propagation of correlations.

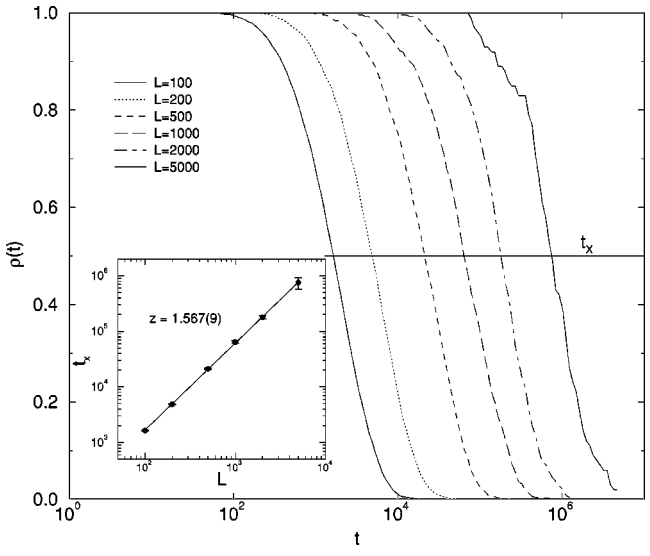

FIG. 4. Dynamic exponent z for the DKCA interface representation. The density $\rho(t)$ of active samples as a function of time for several system sizes is shown, for the symmetric scheme ($p_2=0.5, p_1=0.749$). The horizontal line highlights the value $\rho=1/2$, which corresponds to the crossover time. The inset shows the crossover time $t_\times$ in function of the system sizes. The slope of this curve is the value of the dynamical exponent z. The error bars are calculated considering an error of 1% in the number of samples frozen at a given time.

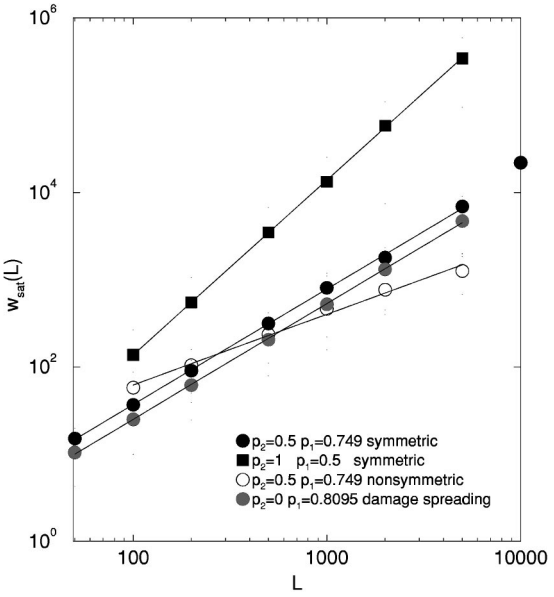

FIG. 5. Roughness exponent α for the DKCA interface representation. Four cases are shown: directed percolation ($p_2=0.5$, $p_1=0.749$ symmetric), directed percolation ($p_2=0$, $p_1=0.8095$ damage spreading), compact directed percolation ($p_2=1$, $p_1=0.5$ symmetric), and nonsymmetric DP ($p_2=0.5$, $p_1=0.749$ nonsymmetric). The line is the power law regression for the data and furnishes the value of the roughness exponent α. The error bars are the standard deviations of the saturation width over realizations at each system size.

A. Symmetric scheme

For the symmetric scheme, our results for the critical exponents agree with the DP values, except at terminal point $p_2=1$ where CDP values were obtained. The critical points (p_2^c,p_1^c) were determined through the growth exponent method [13] (Fig. 3). This method consists in fixing p_2 and varying p_1 until the maximum of the growth exponent β_w is attained.

To determine the crossover time $t_\times(L)$, we plot the fraction of realizations with at least one active site as a function of time (see Fig. 4), and define the crossover time such that half of the initial sample has frozen. The inset of Figure 4 shows the power law behavior of the crossover time; the slope of this line corresponds to the exponent *z*.

To obtain the saturation width, we let all samples evolve to the absorbing state, at a given system size, and determine the final averaged roughness. The exponent α was measured as the slope of $w(L,\infty)$ vs L in a log-log plot. In Fig. 5, we present the results for the saturation roughness in the cases: directed percolation ($p_2=0.5$, $p_1=0.749$, symmetric), directed percolation ($p_2=0$,$p_1=0.8095$, damage spreading), compact directed percolation ($p_2=1$, $p_1=0.5$, symmetric), and nonsymmetric DP ($p_2=0.5$, $p_1=0.749$, nonsymmetric).

In order to verify Family-Vicsék scaling, we use the measured values for the scaling exponents to collapse the width curves at different system sizes to a single curve, as shown in Fig 6. Note the collapse of the width curves, corroborating the Family-Vicék scaling relation.

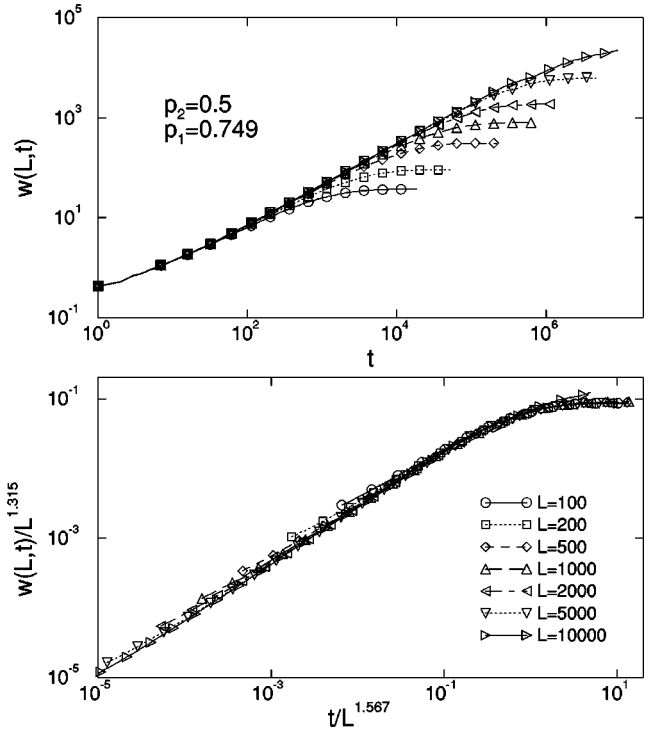

FIG. 6. Family-Vicsék scaling. Upper panel: the width of the generated profiles at different system sizes. Lower: collapse of the curves above using the exponent values measured through numerical simulation at the criticality ($p_2=0.5$, $p_1=0.749$).

It is important to note that the exponents β_w and *z* measured for the chaotic-nonchaotic transition at $p_2=0$ are slightly different from the exponents measured away from this point. This can represent evidence of long-range correlations due the coincidence of the damage spreading and frozen-active transitions at this point, as pointed out by Grassberger [8], but also is consistent to corrections to scal-

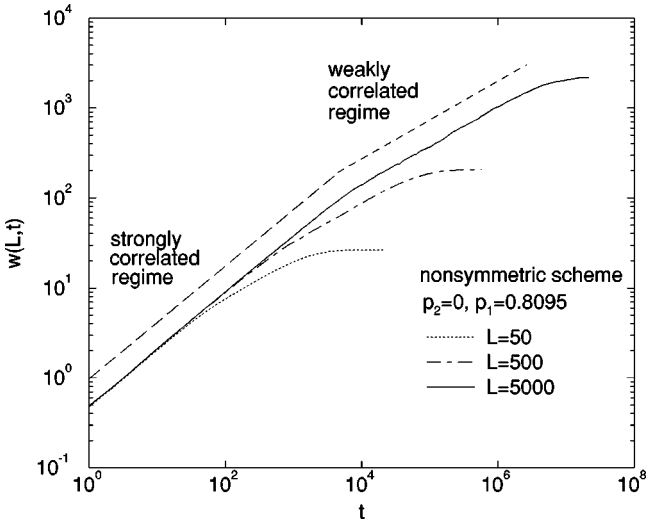

FIG. 7. Profile roughness behavior for a nonsymmetric scheme. Note the two regimes in the $w(L,t)$ vs t curve; for $t \lesssim L$ we have a strongly correlated regime with $\beta_w \sim 0.65$ and for $L<t<t_\times$, a weakly correlated regime with $\beta_w \sim 0.45$.

ing. At this moment we are not able to perform calculations to distinguish these effects.

B. Nonsymmetric scheme

A significant change in the roughening occurs in the nonsymmetric scheme, as shown in Fig 7; we observe two distinct regimes in the roughness growth: a strongly correlated regime, for times $t \lesssim L$, and a weak correlation regime, for longer times. Again, this behavior can be understood by considering the nonsymmetric scheme as deposition in a moving reference frame. The correlations inherent in the dynamics are propagated by the moving reference frame until they reach the system size; then the correlations due the local rules of the automaton take over, decreasing the growth rate of the roughness. These two regimes for the roughness growth implies that is not possible to collapse all the curves using the Family-Vicsek scaling law.

The apparent exponent values measured in the nonsymmetric scheme are markedly smaller: $\alpha \sim 0.92(1)$ for nonchaotic-chaotic and frozen-active transitions; at $p_2 = 1, p_1 = 0.5$, $\alpha \sim 0.984(7)$. As discussed above, the growth exponent presents two values, depending on the roughness growth regime. (The * in the Table I denotes this behavior.) The dynamic exponent z must assume the DP value, as discussed in Sec. II A; in fact, $z \sim 1.6(1)$ for nonchaotic-chaotic and frozen-active (at $p_2 \neq 1$) transitions, while $z \sim 1.9(1)$ at $p_2 = 1, p_1 = 0.5$.

IV. CONCLUSIONS

Growth surfaces generated by the spatiotemporal patterns of the DKCA along its critical lines are studied. The critical roughening exponents, expected to belong to the DP universality class, were measured using power law relations valid at criticality. Except for the terminal point $p_2 = 1$, all the scaling exponents agree with the DP values, in the symmetric scheme, and the scaling law $\beta_w = \alpha / z$ remains valid. At $p_2 = 1$, we confirm CDP values for the exponents. Since the fluctuations in uncorrelated regions are effectively superposed, it is not surprising that the apparent values of β_w and α are smaller in the nonsymmetric scheme. At the nonchaotic-chaotic transition, the exponents measured also agree with the DP values.

ACKNOWLEDGMENTS

We thank the Brazilian agencies CNPq and Fapemig for financial support for this work.

[1] E. Domany and W. Kinzel, Phys. Rev. Lett. **53**, 311 (1984).
[2] S. Wolfram, *Theory and Applications of Cellular Automata* (World Scientific, Singapore, 1986).
[3] W. Kinzel, Z. Phys. B: Condens. Matter **58**, 229 (1985).
[4] P. Grassberger, Z. Phys. B: Condens. Matter **47**, 365 (1982); H.K. Janssen, *ibid.* **42**, 151 (1981).
[5] J.W. Essam, J. Phys. A **22**, 4927 (1989).
[6] R. Dickman and A.Y. Tretyakov, Phys. Rev. E **52**, 3218 (1995).
[7] M.L. Martins, H.F. Verona de Resende, C. Tsallis, and A.C.N. de Magalhães, Phys. Rev. Lett. **66**, 2045 (1991).
[8] P. Grassberger, J. Stat. Phys. **79**, 13 (1995).
[9] H. Hinrichsen, Braz. J. Phys. **30**, 69 (2000).
[10] H. Hinrichsen, Adv. Phys. **49**, 815 (2000).
[11] J.A. de Sales, M.L. Martins, and J.G. Moreira, Physica A **245**, 461 (1997).
[12] J.A. de Sales, M.L. Martins, and J.G. Moreira, J. Phys. A **32**, 885 (1999).
[13] A.P.F. Atman and J.G. Moreira, Eur. Phys. J. B **16**, 501 (2000).
[14] J.A. Redinz and M.L. Martins, Phys. Rev. E **63**, 66133 (2001).
[15] P. Bhattacharyya, Int. J. Mod. Phys. C **10**, 165 (1999).
[16] F. Family and T. Vicsék, J. Phys. A **18**, L75 (1985).
[17] K.B. Lauritsen and M. Alava, Europhys. Lett. **53**, 563 (2001).
[18] A. Vespignani, R. Dickman, M.A. Muñoz, and S. Zapperi, Phys. Rev. E **62**, 4564 (2000); R. Dickman, M. Alava, M.A. Muñoz, J. Peltola, A. Vespignani, and S. Zapperi, *ibid.* **64**, 056104 (2001).
[19] R. Dickman and M.A. Muñoz, Phys. Rev. E **62**, 7632 (2000).
[20] T.F. Nagy, S.D. Mahanti, and C. Tsallis, Physica A **250**, 345 (1998).
[21] A.-L. Barabási and H. E. Stanley, *Fractal Concepts in Surface Growth* (Cambridge University Press, Cambridge, England, 1995).
[22] J.G. Moreira, J. Kamphorst Leal da Silva, and S. Oliffson Kamphorst, J. Phys. A **27**, 8079 (1994).
[23] J. Kertész and D.E. Wolf, Phys. Rev. Lett. **62**, 2571 (1989).
[24] I. Jensen, J. Phys. A **29**, 7013 (1996).
[25] J.M. López, Phys. Rev. Lett. **83**, 4594 (1999).